

Fault Location using Artificial Neural Network in a Radial Electric Power Distribution System with Recloser and Sectionalizers

EZE COSMAS CHIBUZO¹, ASHIGWUIKE EVANS², EJIMOFOR CHIJOKE³
^{1, 2, 3}*Department of Electrical and Electronic, University of Abuja, FCT, Nigeria*

Abstract- Promptly locating and clearing faults is key to maintaining the reliability of the power grid. The traditional way of locating faults on the grid cannot be relied upon due to the high costs involved with dispatching repair crew to search for the location of the fault and the time involved in achieving that. While the installation of protective devices such as reclosers and Sectionalizers help in protecting the network and preventing blanket outage of the network when a permanent fault occurs, they by themselves cannot locate the point on the network where the fault has occurred. However, the transients launched by the inception of a fault on the line contain features that could be used to trace the location of the fault. The main aim of this study is to employ artificial neural networks in locating faults in a distribution system involving reclosers and Sectionalizers. The data for training the artificial neural network is to be obtained by simulating various fault scenarios in MATLAB/Simulink and the features of the data are extracted by processing the data using the discrete wavelet transform (DWT). The modelling and simulation of the fault location system is done in MATLAB/Simulink on a 15 bus IEEE distribution network with a grid supply and a distributed generator connected to the system. Twenty (20) random trials were conducted on different lines of the network and the fault location system was able to identify the faulty line 60% of the times..

Indexed Terms—Artificial Neural Network (ANN), Discrete wavelet Transform (DWT), Fault, Recloser, Sectionalizer.

I. INTRODUCTION

Abstract: Reliability is a key aspect of the power grid, which may be managed by pre-emptive measures or

by fault location. Pre-emptive measures are implemented through the incorporation of redundancy in pathways and with equipment which require huge investments in order to avoid outages. Fault location on the other hand decreases the process time for fault clearance [1]. One effective way of improving distribution system reliability is the placement of switches and protective equipment in optimal locations [2]. This is typically implemented through the deployment of reclosers and Sectionalizers.

Although the electric grid is designed to continuously supply power to consumers in an efficient and reliable manner, it is prone to faults which could lead to interruption in the supply of electricity [3]. A fault could be referred to as an unpermitted deviation from the standard operation of the system which may be temporary or permanent. A temporary fault is self-resolving within a specified time interval and does not lead to permanent damage on any components in the network. Permanent faults exceed the time limit for temporary faults and result in the damage of one or several components in the network that need to be repaired before the service can be restored [1]. Temporary faults can be resolved through the action of reclosers which are switches, like circuit breakers, but intelligent enough to test the line for any fault and disconnect the line temporarily for a short period of time to clear the fault [4] [5]. Where the fault persists and becomes permanent thereby requiring repairs, the faulty portion of the network is sectionalised or isolated from the healthy portion of the network pending the repairs and restoration by the utility company.

The fault location process involves a number of steps that is initiated by the occurrence of a fault in the network. The steps involved in fault location are: fault detection, fault area determination, general fault location, fault isolation/clearing and service restoration. When forced outage occurs in an electric

network with reclosers and Sectionalisers, the fault location process would traditionally involve an affected customer calling to inform the utility company of the outage and a team is dispatched to trace and locate the fault, classify the fault and clear it. The disadvantages of this process are; delayed reports, fake reports and the fact that tracing the location where the fault occurred can be a herculean and time-consuming task especially in networks covering large areas which may also require knowledge and experience of the area [1]. The advent of microprocessor based intelligent monitoring and data acquisition systems has enabled fault location through data analysis which can be categorised into the following: Impedance based, travelling wave techniques and knowledge-based approach. The cost effectiveness of impedance-based methods of fault location is the reason for their wide acceptance and application in distribution systems. This method requires only the data for voltage, current and line impedance which is typically obtained at the primary substation level and uses the fundamental frequency to approximate the location of the fault [1].

The occurrence of a fault in a line creates a high frequency wave of current and voltage. These travelling waves propagate away from the fault towards both ends of the line in the form of electromagnetic pulses. The discontinuities in the network such as short circuits, open circuits and line terminals cause the wave to experience reflections and refractions as they propagate. This continues until a steady state is attained where the energy of these travelling waves gets completely dissipated [6]. Line terminals installed at each end of the line or network can be used to record the travelling time of the wave from the fault location to each of the terminals and given that the recording times are synchronized at the two terminals, the detection time between the two waves can be determined. Traveling-wave methods are of three types which are: A, B and C type. Types A and B methods rely on the traveling-wave signal generated by the fault and returning to the measurement point. Methods A and B both require detection devices, which detect the signal(s) from the fault. A-type methods are reliant on one-end measurements while B-type require a reader at each end of the line, which makes it unattractive in distribution networks. In C-type on the other hand, a

traveling-wave is introduced in the system which is used to calculate the fault location [7]. This injection of a travelling wave into the system reduces the need for continuous high resolution data acquisition. [7]

Knowledge-based approach falls under soft computing in contrast to traditional hard computing where precision is sought. Hard computing relies on the ability of computers to perform large amounts of computations at high speeds through algorithms that operate serially, are controlled by a central processing unit (CPU) and store the information at a particular location in memory. Soft computing on the other hand mimics the information processing method of the human brain which relies on distributed representations and transformations that operate in parallel, have distributed control through interconnected processing elements or neurons and stores the information in various straight connections called synapses. In soft computing there are higher possibilities of finding complex correlations because the restrictions are looser but the accuracy and certainty come at a price which result in a trade-off between precision and uncertainty [8]. There are three broad areas under knowledge-based approaches which are: Expert systems techniques, Artificial neural networks and Fuzzy-logic systems [1]. Artificial neural networks have high accuracy in fault location as confirmed by [9], [10], [11], [12], [13], [14], [15], [16], [17], [18], [19], [6], [20]. This work would focus on the use of Artificial neural network to locate faults in a distribution network with Reclosers and Sectionalisers. This work would focus on the distribution section of the grid network as the analysis of the failure statistics of most utilities indicate that the distribution system is the most affected by faults [21]. Also, switches and other protective equipment placed at optimal locations in the distribution network form part of the protection system of the network and help to improve the reliability of the system [2]. As such, Reclosers and Sectionalisers would be included in the system modelled in this project. The modelling and simulation for this work would be carried out in MATLAB/Simulink

II. LITERATURE REVIEW

A fault in a distribution network can be referred to as

an unpermitted variation from its normal operating conditions. A number of reasons could be responsible for this anomaly which include: electrical lines coming in contact with each other creating a short circuit, the coming into contact of electric lines by animals or vegetation etc [1], [25]. The traditional way of locating and clearing faults in an electric grid system involves the affected customer calling the utility company to register a complaint of an interruption of service. The utility company in response to the complaint would be tasked with the responsibility of tracing the location of the fault and clearing the fault to restore the service [1]. This method is time consuming and requires much effort on the part of the restoration team of the utility company. While protection relays such as reclosers and Sectionalisers may be used to indicate the general area defined by a protection zone, fault locators are used for pinpointing the fault location with a high degree of accuracy [26]. With data acquisition systems such as SCADA, a fault can be located based on certain patterns or features in the fault data. The fault data is obtained from measurements of voltages and currents in the line at the inception of the fault. [26] identifies the basic fault models that must be considered in the formulation of a fault location algorithm. These basic linear fault models are depicted in Figure 2.1 and listed below as:

Phase to earth fault

Phase to phase fault

Two phases to earth fault

Three phases fault

Three phases to earth fault

Broken conductor fault

Phase to earth fault with broken conductor

Broken conductor with phase to earth fault

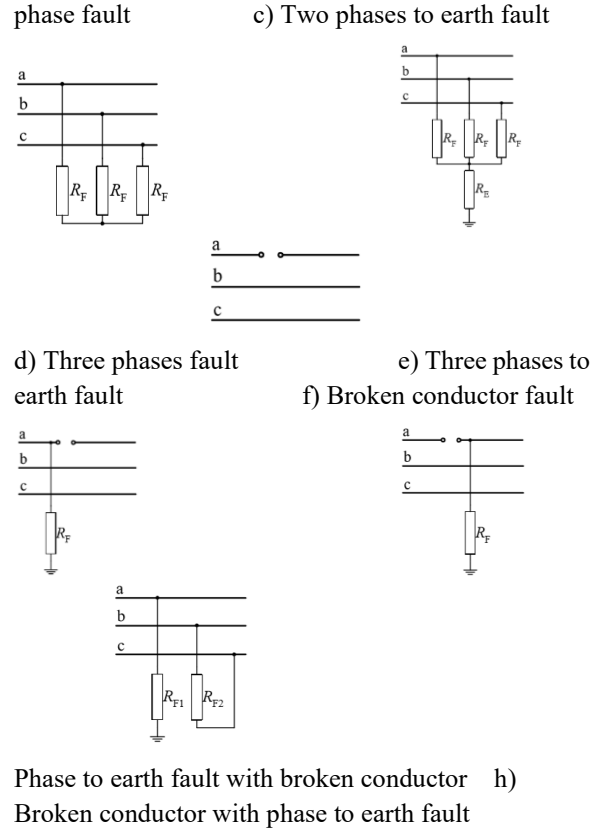
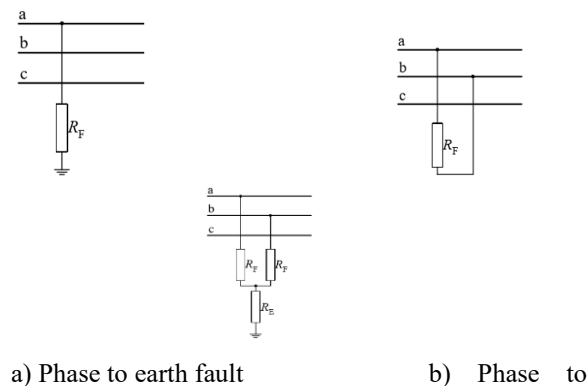


Figure 2.1: Fault Models [27]

Fault Location Methods

Recent research in fault location have been applied to HVDC systems as seen in the work of [28], [29], [30], [31], [32], [33], [34]. This is because the modern smart grid is progressively aligned for direct current power transmission [31]. Never the less the methods used to formulate fault location algorithms are similar to those for the conventional alternating current transmission system. These methods can be classified into three broad categories which are; the travelling wave method, the impedance-based method and the knowledge based or artificial intelligent techniques [1], [35].

Travelling Wave Method for Fault Location

Travelling wave-based methods associate characteristic frequencies linked to travelling wave paths with the location of the fault. The reflections and transmissions of the waves generated when a fault appears are the basis for locating the fault using this method [35], [36]. These waves travel in both

directions from the point of the fault as shown in Figure 2. The waves launched by a fault have energy over a wide spectrum with the 20kHz to 2MHz range being mostly the useful range for travelling wave fault location [37]. Travelling wave techniques are of three types: type A, type B and type C. Both types A and B rely on the returning travelling wave signal from the fault and require detection devices to detect the traveling waves. Type B requires a signal reader at each end of the line which makes it unattractive for distribution networks while type A requires only one end measurement. Type C introduces a travelling wave in the system which is used to compute the fault location. If the recording signals are synchronized at terminals 1 and 2 of the line in a type B travelling wave fault location method for example, then the time it takes the wave to travel from the fault to each terminal can be recorded. The difference in detection times can be determined as shown in equation 2.1 [1].

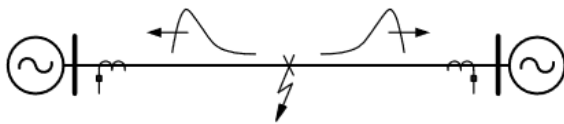


Figure 2.2: Travelling wave fault location system [36]

$$t_d = t_1 - t_2 \quad \dots 2.1$$

Where t_d = difference in recording time between terminal 1 and 2

t_1 = recording time at terminal 1

t_2 = recording time at terminal 2

Given that the length of the line L is known and the velocity of the wave C is known, the distance to the fault d can be calculated as shown in equation 2.2.

$$d = \frac{L - Ct_d}{2} \quad \dots 2.2$$

The concept above depicts the main principles underpinning the traveling wave method of fault finding which is often used in transmission networks to accurately locate a fault on the line. This method is not feasible in a distribution network due to the branched configuration of the grid and additional signal processing tools such as wavelet transform and filtering may be required to simplify the computations of the wave [1], [38]. Where filters are employed with only one line recording terminal as in type A, the fault signal and the subsequent reflections can be singled

out among the frequency peaks and the time difference used to calculate the fault location. [37] and [39] also suggest the use of a reference event such as an automatic reclosing without fault along with the travelling waves captured during a fault to compute the fault location. The drawback with this is that type A fault signals are difficult to detect when the fault occurs close to the terminal [1]. In type C, the fault location can be evaluated as shown in equation 2.3.

$$L = \frac{C(t_2 - t_1)}{2} \quad \dots 2.3$$

Where L = distance to fault

C = velocity of the wave signal

t_1 = the signal injection time

t_2 = the signal return time

In a meshed layout, this method could give rise to several possible fault locations. A possible solution to this is the injection of a DC signal and the used of Hall Effect sensor technology to detect the signal returning through the ground [1].

The authors in [40] proposed a novel travelling wave fault location method based on directed tree model and linear fitting to solve the problem of inaccurate fault location in transmission network due to anomalies such as travelling wave location device faults, startup failure and time recording error. The location error in this work is 0.01% for any fault type and location. This method involves graphical analysis and requires detection devices with high speed in the range of less than 1µs.

The authors in [41] proposed a new method for fault location in resonant grounding systems based on variable modal decomposition (VMD) and Kurtosis calibration. The feature of the fault signal is extracted by decomposing the fault signal into intrinsic mode functions (IMF) using the VMD algorithm with adaptive characteristics and the IMF with transient fault characteristics are accurately selected. The arrival time of the travelling wave head is detected using the discrete kurtosis value which is calculated for the IMF component with the highest frequency. The wave head is calibrated by noting the time corresponding to the maximum kurtosis value which is the travelling wave head moment. The simulation results from this study showed that this proposed method can accurately calibrate the wave head and achieve the desired fault location.

The authors in [42] proposed a novel protection and fault location combined algorithm for mixed overhead lines and underground cable system. The proposed method applies the Morphological Gradient (MG) to the modal component of synchronized measured currents at both ends of the mixed transmission line to detect the transient components generated by a fault. The sign of superimposed components is used for discriminating internal and external faults and the fault location is computed using the difference between the times related to the transient components. The simulations were carried out using the EMTP-RV software with a sampling frequency of 1.5MHz. Analysis of the current signal and the fault location algorithm were implemented in MATLAB.

The authors in [43] proposed a cable fault location method in VSC-HVDC system based on improved local mean decomposition. This was aimed at solving the problem of low positioning accuracy caused by modal aliasing and noise interference in DC cable fault location analysis of a VSC-HVDC system. This work involved the use of a double-ended fault location method for flexible DC cables based on improved local mean decomposition (LMD). The product function (PF) component is obtained by decomposing the six-mode voltage signal using the local mean decomposition (LMD) and then to overcome the problem of the instantaneous frequency of the LMD being limited by the extreme value, the Hilbert transform is performed on the PF1 to obtain the instantaneous frequency curve, and the arrival time of the voltage traveling wave head is determined from the mutation information. The fault distance is thereafter obtained by using the double ended travelling wave fault location principle. Various fault conditions were simulated, analysed and compared with wavelet transform and Hilbert–Huang transform. A positioning error within 1% was obtained from the results which shows that the proposed method is less affected by interference noise and transition resistance.

Impedance Based Method for Fault Location

The data for line impedance, voltage and current are all that are required for fault location using the impedance-based method. The fault location is approximated using the fundamental frequency and the aforementioned data which are typically usually collected at the primary substation level [1]. This

method is widely used in distribution systems due to their cost effectiveness. Owing to the presence of dispersed loads, the computations are initiated in the first line section and then carried out sequentially in the network to determine the fault steady state conditions for all the sections. This analysis can either be done with symmetrical components or in phase domain. The choice of phase domain in this case is recommended because unbalanced loads are common in distribution systems [1]. Impedance based methods generally solve the line equations iteratively with an initial guess of the distance. The calculations are repeated for the next section if the fault distance is calculated to be beyond the segment and is continued in this fashion until the fault location falls within the range of the conductor [1]. A simplified formula for a single ended impedance-based method is presented in equation 2.4.

$$V_s = d \cdot Z_{L+} \cdot I_s \quad \dots 2.4$$

Where, d = distance to fault

Z_{L+} = Positive sequence line impedance

V_S = Voltage measured at the relay

I_S = Current measured at the relay

Lateral branching is a common feature in distribution systems and as such, they need to be accounted for in the computations. This can be achieved by computing the equivalent paths corresponding to the number of laterals. Larger scale systems could employ a method where the equivalent node impedances are computed through a power flow analysis before the occurrence of a fault [1].

To obtain reliable results, it is important to properly consider the assumptions and details in the line and load parameters. In a distribution network with shorter lines, the capacitance may be considered negligible but in a network with longer lines, the capacitance has to be accounted for. Although difficult to estimate due to the fact that they are usually obtained from historical data, the load data also needs to be considered. A poorly approximated load profile does not really affect the system to a large extent since the load current is much smaller than the fault current. However, in cases where the fault resistance is higher, the value of the load current and the fault current become closer and therefore a poorly approximated load increases the inaccuracy of the results [1].

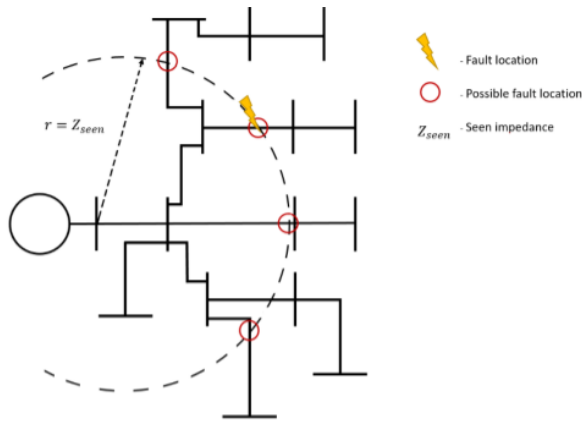


Figure 2.3: Typical branched distribution system showing the multiple estimation problem where the fault distance is represented by the dashed circle [44]

A number of possible fault locations can be identified since the method involves multiple estimations. The impedance is calculated in the network as seen from the measuring point and all points with impedance equal to the assumed fault impedance are identified. Due to the branched layout of distribution grids, multiple points with the same impedance are obtained as shown in Figure 3. There are two ways to handle the multiple estimation problem. One solution is by analysing the waveform recorded at the substation, which displays the characteristics of the present protective devices before the fault. As a consequence, the fault is located at the point, which has the same upstream protective devices. If two or more points have the same preceding protective devices, a comparison can be made between the main feeder current and the sum of the affected load currents for each possible point. Another solution is the installation of fault indicators which detect and get triggered at the presence of fault currents, and analysing the load currents in the unaffected lines [44].

Impedance based methods can be subdivided in two main categories: one-end measurements and multi-end measurements. The one-end measurement method solely relies on voltage and current measurements at one location; commonly at the beginning of the line. Multi-end methods on the other hand require measurements at several nodes; the minimum being at every consumption and production node in the system [1]. The two categories have apparent pros and cons. One of such is the increased number of installations of

a multi-end method compared to a lower level of accuracy of a one-end method. Other less obvious differences are the ability to perform in a grid structure incorporating distributed generation. The accuracy of one-end method is affected by distributed generation while multi-end methods are not affected by distributed generation [45]. The effects of distributed generation are further magnified with higher generation capacity installed coupled with greater distances from the distributed generation source [45]. The authors in [46] affirmed the effect of the load model on the steady state of the power distribution system which in turn will directly influence the fault locator performance.

The authors in [47] proposed a method for fault location in distribution network by solving the optimization problem based on power system status estimation (PSSE) using a phase monitoring unit (PMU). Two objective functions are designed to identify the faulty section of the line and the fault location is based on computing the voltage difference between the two ends of the lines. The proposed algorithm combines the PMU in the PSSE problem in order to estimate the voltage and current quantities at the branch point and the entire network nodes after the occurrence of the fault. The results from this study showed that the proposed algorithm was able to determine the location of the fault with a maximum error of 1.21% at a maximum time of 23.87 seconds.

The authors in [48] proposed a fault location method which uses voltage sag measurements for advanced fault location and condition-based monitoring. The method was shown to have good potential for permanent and temporary fault location on overhead radial distribution system and has been deployed on feeders located mainly at Hydro-Quebec and a couple of other Canadian cities. In this method, the fault generates a high current that is a function of the impedance between the source and the fault as well as the type of fault. This fault current causes a voltage dip which is used along with the fault current, the phase angle of voltages and a triangulation technique to compute the fault location.

A novel noniterative single-ended phasor domain fault location method with distributed parameter model for AC transmission lines. was proposed by the authors in [49]. The proposed method leverages the additional information brought by the operation mode of circuit

breakers and as such only requires the local measurements and does not require the measurements and the equivalent source parameters of the remote system. Furthermore, the proposed method only uses single-ended data and is not affected by communication and synchronization. It is a non-iterative method with no risk of non-convergence. The effectiveness of the proposed method was verified through several case studies in PSCAD/EMTDC, with different fault types, fault locations and resistances.

The different categories of impedance-based methods offer different approaches which have different pros and cons. Collecting information about the topology of the network, available data, presence of distributed generation, accuracy and time requirements are a good way to guide one's choice [1].

Artificial Neural Network Based Fault Location

Artificial Neural Network methods for fault location fall under a broad category which is known as knowledge-based approaches. Three sub-categories exist under the knowledge-based approaches which are; expert systems techniques, artificial neural networks and fuzzy logic systems [1]. The knowledge-based approaches reduce the real time computational burden of the system.

Artificial neural networks are taught by examples as opposed to expert systems which are rule-based. Artificial neural networks require training using a large set of data representing various fault scenarios in order to provide reliable results. They can be trained to recognize and map complex inputs of voltage and current levels; fault distance with continuous data [1]. Consequently, for a given network topology, data from a wide range of fault scenarios for the network needs to be available and updated with any change in topology. In cases where the area is newly established, these data may be unavailable and grid expansions may cause problems with the performance of the model [44]. However, manufactured data could be used in the training of the artificial neural network model but could increase the possibility of uncertainty if excessively implemented [1]. The main advantages of artificial neural networks are their ability to generalize and derive new unseen input-output matches along with their speed and accuracy. The main disadvantages of artificial neural networks are the large amounts of data of simulated or actual fault

scenarios required to train the network and the fact that the process of training needs to be repeated if any change occurs in the network thereby making the model maintenance intensive in a dynamic network where changes occur continuously.

Different types of faults at varying short circuit and loading levels are characteristic of distribution systems as a result of their usual multiple branches with different characteristics. This may increase the difficulties involved in determining the complex connections and the fault location. To solve this problem, the authors in [44] proposed the use of support vector machines (SVM) to break up the complexity by classifying fault types and short circuit levels and assigning an artificial neural network to each category.

The authors in [50] developed a method for remote fault identification and analysis in electrical distribution network using artificial intelligence. The work presented wavelet and machine learning-based approaches for distinguishing different faults that occurred at different locations in a radial power distribution network. Wavelet decomposition-based detail coefficients along with their Kurtosis and statistical nature were used to analyse fault currents. Six different machine learning methods were used and tested with random unknown data in time series. The best method giving the highest accuracy in most cases was found to be the decision tree method.

The authors in [51] proposed a new method for fault detection and classification in a renewable microgrid. The method first enhances fault detection performance in microgrids characterized by nonlinear relationships which include photovoltaic, hydrokinetic, and variable electric load systems. Next, a robust method for fault detection and classification is provided by the combination of the discrete wavelet transform with various types of neural networks and supervised learning techniques. The proposed method was evaluated using an IEEE-5 feeder test bed representing a realistic ring network configuration. The results yielded a low prediction error of 1.31×10^{-31} which show that the radial basis function neural network model exhibited promising outcomes, thereby highlighting its practical potential for enhancing system reliability and performance. Furthermore, several test cases were conducted by altering the ground resistance to train the neural networks,

demonstrating the effectiveness of this neural network in accurately identifying fault conditions.

The authors of [52] presented an off-line continuous wavelet transform and machine learning method for accurately localising faults of the DC-side in Voltage Source Converter (VSC) based Multi-Terminal Direct Current (MTDC) networks utilising optically-multiplexed DC current measurements sampled at 5 kHz. Commercially available equipment was used to evaluate the technical feasibility of optically-based DC current measurements through laboratory experiments. MATLAB/Simulink based analysis was used to test the proposed fault location algorithm in different fault scenarios and locations along the simulated DC grid. The results obtained revealed that the proposed fault location scheme can accurately identify the type of fault and compute its location. The scheme was also found to be effective for faults with high resistances of up to 500Ω. It was revealed by further sensitivity analysis that the proposed scheme is relatively robust to additive noise and synchronisation errors.

[53] presented a fault classification and location algorithm for medium voltage overhead lines with load taps and embedded remote-end source. This fault classification and location algorithm was based on artificial neural-network (ANN) utilising the frequency spectra of the sampled voltage and current signals recorded by the digital relay at the substation. The feature extraction was carried out using the fast Fourier transform (FFT) of the current and voltage signals. Classification and location of shunt faults on a medium voltage distribution network was done using a multilayer perceptron neural network with the standard back propagation technique. Training and testing of the ANN was done using the results obtained from simulating a 34.5kV overhead distribution system in MATLAB/Simulink. The results obtained were satisfactory for locating faults on radial overhead distribution systems with load taps and in the presence of remote-end source connection.

[54] developed an artificial neural network-based fault location system for locating double phase to earth fault on non-direct ground in a transmission line. The system uses the GPS to locate the position and the GSM to communicate the position to a system supervisor. The generated current and voltage waveform signals were sampled at a frequency of

720Hz to extract the feature for processing. The neural network system trained to diagnose double faults was found to accurately diagnose abnormal operation resulting from simultaneous multiple faults.

Reclosers and Sectionalisers in Fault Location

The optimal placement of auto-reclosers and remodelling the distribution system can be used to improve system reliability and efficiency [55], [56], [57], [58], [59], [60]. A recloser or auto-recloser is a protective device that protects upstream load points from downstream faults. A recloser locks out and isolates a permanent fault from the rest of the grid after a predetermined number of reclosing operations [57], [59]. In doing so, the recloser improves the reliability by preventing a sustained outage in a what is known as a fuse saving technique employed in distribution utilities where the fault is interrupted to prevent the melting away of the fusible link in an expulsion fuse and then reclosed to restore power to the healthy portion of the network [61] [57], [62]. This technique is effective because most overhead line short circuit faults are temporal and usually clear themselves [63], [61], [64]. Unlike the recloser, the Sectionalizer cannot operate during a fault but rather works in coordination with an upstream recloser. The Sectionalizer promptly and automatically isolates the faulty part of the network when a permanent fault occurs [57]. The cost of installing reclosers and Sectionalisers is non-trivial and therefore there needs to be an optimum means of determining the settings, number and locations where they need to be installed as seen in the literature [57], [59], [60], [65], [66].

Most of the literature do not explicitly mention the use of reclosers and Sectionalisers in precise fault location apart from their usual function of maintaining the continuous supply of power to consumers. [67] proposed a fault location and isolation method for distribution networks based on adaptive reclosing. The goal of the authors was to avoid multiple reclosing by being able to distinguish temporary and permanent faults thereby preventing momentary outages to the upstream part of the network and saving the contact life of the switches. Pang in [68] proposed an information fusion-based fault location method for distribution network to mitigate the problems associated with losses or faults in the information from the distribution substation. The method employed in this work [68] creates one information matrix based on

the action of all the protective relays when a fault occurs and another matrix is created based on the wave data of the current recorded at the foot node. Both information matrices are combined using D – S evidence theory to locate the fault.

The penetration of distributed generation (DG) in conventional power systems brings up issues in the coordination of protection devices due to the fault current contribution from the DG [58], [62] [64]. Some of the frequent issues encountered by the addition of DG to the distribution networks are; blind protection, sympathetic tripping and failure of reclosing. To solve this problem, the authors in [58] focused their research on the impact of reclosers on overcurrent relay blind protection areas with distributed generators (DG) embedded in the distribution network. A non-operation or delay in the over-current relay with fault point impedance may be caused by the blind protection issues as a result of the relay feeder pickup current. The authors in [58] proposed a recloser to avoid blind protection due to the addition of DG to the distribution network as opposed to the conventional solution of increasing the relay sensitivity.

[62] proposed a relaying scheme targeted at microprocessor based reclosers for fuse saving under transient conditions. A relay operating characteristic is defined based on voltage and current magnitudes obtained at the recloser location. The reclosing delay resulting from the DG fault contribution is compensated for by the voltage term in the relay characteristic. The relaying scheme is independent of the number of distributed generators (DG) and makes no use of communication links. Furthermore, the new scheme was shown to maintain proper recloser-fuse coordination for different fault conditions and DG configurations.

Discrete Wavelet Transform

The discrete wavelet transform is a signal processing method that quantifies the energy that is contained within specific frequency bands at particular periods within a signal. The wavelet transform is more appropriate for analysing transient signals due to the fact that fault transients are non-stationary and there is the need to analyse them at various transition periods as the signal changes [69]. Wavelet transforms employ a variable window size and are capable of multiple

resolutions in time and frequency.

The wavelet transform is based on the transformation of the transient signal into a series of parameters called approximation and detail coefficients which represent the slow and fast changes in the signal.

The discrete wavelet transform (DWT) of a signal can be found using equation 2.5 [70]. This is done by passing the signal to be transformed through a series of low and high pass filters to decompose the signal into a series of approximate and detail coefficients.

$$DWT(m, n) = \sum_{-\infty}^{\infty} x(t) * \Psi_{m,n}^*(t) dt \quad \dots 2.5$$

Where, $\Psi_{m,n}^*(t)$ is the mother wavelet and $x(t)$ is the signal to be transformed. The value of $\Psi_{m,n}^*(t)$ is computed using equation 2.6 [70].

$$\Psi_{m,n}^*(t) = \frac{1}{\sqrt{a_0^m}} * \Psi\left(\frac{t - na_0^m b_0}{a_0^m}\right) \quad \dots 2.6$$

‘m’ represents the discrete steps of the scaling parameter or level which determines the wavelet frequency;

‘n’ represents the discrete steps of the translation parameter or the position;

‘*’ denotes complex conjugate.

The scale parameter $a = a_0^m$ and the translation parameter $b = na_0^m b_0$

where $a_0 > 1$ and $b_0 > 0$ in finding the DWT of the signal $x(t)$.

Microprocessor Relays

Protection relays play an important role in electric power systems and have been around for a long time. Originally, protection relays were of the electromechanical type which operated based on the principles of electromagnetic attraction or electromagnetic induction [71]. These provided overcurrent, overvoltage, differential and distance protection functions. The development of solid-state technologies and the microprocessor brought about many improvements in distribution protection such as; lower costs, higher reliability, improved protection and control and faster service restoration [72], [73]. Despite the development of complex control and protection algorithms for the microprocessor or digital relay, they were not implemented in those early microprocessor relays but only performed basic relay

functions while taking advantage of the hybrid analogue and digital techniques [71]. Over time however, there have been more improvements on the hardware and software of microprocessor relays and sophisticated algorithms employing artificial intelligence techniques such as neural networks and adaptive protection are being implemented in microprocessor relays [71].

III. RESEARCH METHODOLOGY

Recloser and Sectionaliser Modelling

Reclosers and Circuit breakers are normally equipped with reverse-time overcurrent relays of a characteristic given in equation 3.1.

$$t(I) = \left(\frac{A}{M^P - 1} + B \right) \times TD \quad \dots 3.1$$

Where,

A, B and P are constants for a particular curve characteristic.

t is the operating time of the recloser.

M is the ratio I_{sc} / I_{pickup} (I_{pickup} is the recloser current setpoint and I_{sc} is the short circuit current)

TD is the time dial setting.

Equation 3.2 is typically implemented in a block with an appropriate inverse-time characteristic.

$$t(I) = \left(\frac{28.2}{(I_{sc} / I_{pickup})^2 - 1} + 0.1217 \right) \times TD \quad \dots 3.2$$

The timing diagram for the coordination of the recloser and Sectionaliser is depicted in Figure 3.1 and Figure 3.2.

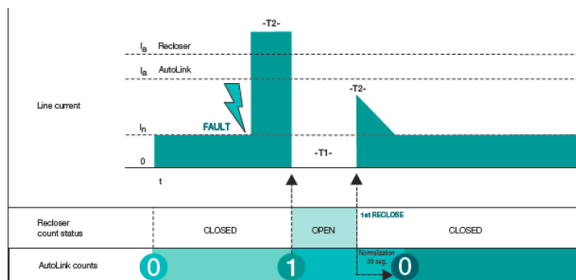


Figure 3.1: Typical Recloser and Sectionaliser operation under temporary fault condition [74]

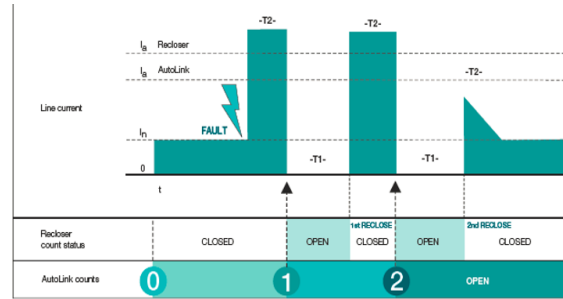


Figure 3.2: Typical Recloser and Sectionaliser operation under permanent fault condition [74]

The recloser model in this work incorporates the following blocks:

Measurement section: This section measures the root mean square value of the instantaneous current passing through the recloser. A schematic of the implementation of this block is shown in Figure 3.3.

Comparator section: This section compares the current thresholds with the programmed values as depicted in Figure 3.3.

Logic and Counter section: This section counts the delay periods required before operating the circuit breaker based on the time-current characteristics. The equation for the time-current characteristics is given in equation 3.2. The relay block in this section outputs a Boolean value to actuate the circuit breaker. If the current is less than the recloser setpoint value, the output is zero (0); if the current is greater than the setpoint value, the output is one (1).

Actuating section: This consists of the circuit breaker that does the function of opening or closing the line as required.

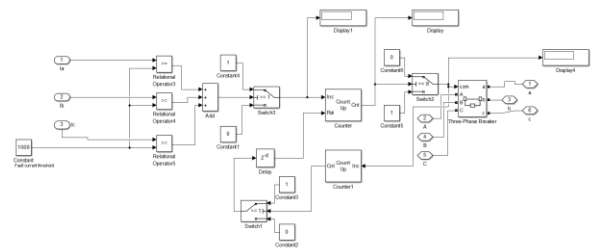


Figure 3.3 shows the schematic representation of the recloser implemented in Simulink in this work.

Figure 3.3: Recloser Implementation

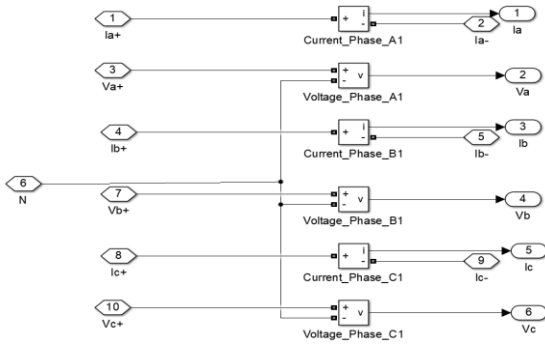


Figure 3.4: Measurement Block

Sectionalisers operate after a predetermined number of reclosing operations for permanent faults. When the line current attains a value of 10% above the preset actuating current, the Sectionalisher begins counting the opening operations of the upstream recloser indicated by a zero current flow sensed in the line. From the operation of the upstream recloser, a counter in the Sectionalisher counts the number of reclosing attempts and when the trip count has been reached, the Sectionalisher trips off the supply to the faulty section of the network. If the recloser recloses the circuit and no fault is detected within the memory resetting time, the counter resets and returns to monitor mode. Figure 3.5 shows the schematic representation of the Sectionalisher implemented in Simulink in this work. The Sectionalisher implemented for this work isolates the faulty portion of the network when the fault persists after the first reclose attempt.

The Sectionalisher block in this work incorporates the following blocks:

Measurement/comparator block: This block measures the rms values of the line currents

Counter section: This section counts the number of reclosing attempts on the line and signals the actuating block when the predetermined number of counts have been reached

Actuating section: This consists of the circuit breaker which isolates the line when the number of recloser counts has been attained.

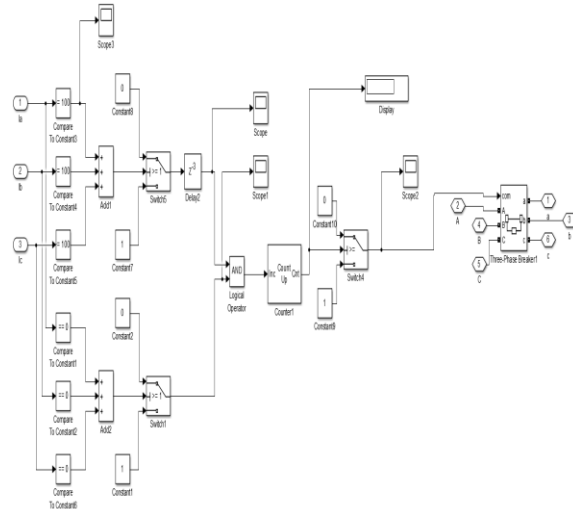


Figure 3.5: Sectionalisher implementation in Simulink Test Feeder Modelling

The test feeder is modelled in MATLAB/Simulink around a standard 15 bus IEEE test feeder distribution system developed by [75].

Feeder Parameters:

Main source => 1 (3MVA, 3-phase short circuit level at base voltage)

Base voltage => 11kV

Number of lines => 14

Number of buses => 15

Number of loads connected => 14

Number of distributed generators connected => 1 (6MVA, 3-phase short circuit level at base voltage).

Figure 3.6 shows the test feeder used in this work.

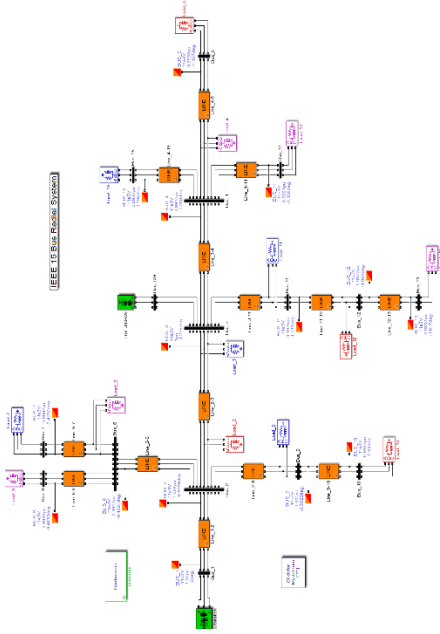


Figure 3.6: IEEE 15 Bus Test Feeder [75]

For analysis the feeder is divided into zones and sections. Zone 1 has two sections; Section 1 and Section 2. Zone 2 has Section 1 and Section 2 as well. Table 3.1 shows this grouping.

Table 3.1: Grouping and organisation of the distribution feeder lines

Zone	Section	Lines	Serial Numbers
1	1	Line 1-2, Line 2-3, Line 2-9, Line 2-6	1, 2, 3, 4
1	2	Line 9-10, Line 6-7, Line 6-8,	10, 11, 12
2	1	Line 3-4, Line 3-11, Line 11-12, Line 12-13	5, 6, 13, 14
2	2	Line 4-5, Line 4-14, Line 4-15,	7, 8, 9

Data Collection and Processing

To generate data for training the artificial neural network, current and voltage sensors are placed upstream close to the generator substation to record samples of the instantaneous voltage and current of the

feeder under the various fault conditions. The sample size covers the period from the inception of the fault up to the point of sectionalisation of the faulty portion of the network. The current and voltage data are processed using the DWT algorithm. Appendix III shows the Simulink setup used to generate the data. The fault block is connected to the lines one after the other and all the possible fault scenarios are simulated to generate the data.

Feature Extraction

The features obtained from performing the discrete wavelet transform (DWT) on the voltage and current wave data are used for the neural network that locates the fault position on the line. The wavelet transform is done on the portion of the waveform where the fault occurred. The transient signal waveform is sampled at 1kHz. The span of the fault signal is taken from the instant the fault is initiated up to the moment the faulty portion of the network is sectionalised. This time span amounts to 125ms. The sampled data is fed into a Simulink buffer to receive the discretised samples and thereafter fed into the DWT block for transformation to extract the features from the resultant approximate and detailed coefficients. The number of samples fed into the DWT block through the buffer in Simulink is given by equation 3.3. The inputs to the DWT block are interpreted as frames whose sample size must be a multiple of $2^{N_{levels}}$. In this work a frame is realised using a buffer set to hold 64 samples of the voltages and currents. The asymmetric tree structure and single output is used for the DWT block used in Simulink.

$$\text{No. of samples} = \frac{125 \times 10^{-3}}{1 \times 10^{-3}} = 125 \quad \dots 3.3$$

These features for every simulated fault condition would be fed to the artificial neural network along with the target binary data for training the artificial neural network. The choice of the wavelet is the Daubechies 5 wavelet and the number of decompositions done is obtained using equation 3.4 [76]. The operation ‘int’ in this case means integer of the expression in the bracket.

$$N_{levels} = \text{int} \left(\frac{\log(f_s/f_e)}{\log 2} \right) + 2 \quad \dots 3.4$$

Where $f_s = 1\text{kHz}$ and $f_e = 50\text{Hz}$, the number of decompositions or levels is given as shown in equation 3.5.

$$N_{\text{levels}} = \text{int} \left(\frac{\log(1000/50)}{\log 2} \right) + 2 = 6 \text{ levels}$$

...3.5

Since the high frequency signals are characteristic of the fault signal, the RMS values of the detailed coefficients of the DWT are used as the features of the fault signal. This is given in equation 3.6 [76]. Where x_i is a sampled measurement and n denotes the number of measurements or samples.

$$\text{RMS} = \sqrt{\frac{1}{n} \sum_i x_i^2}$$

...3.6

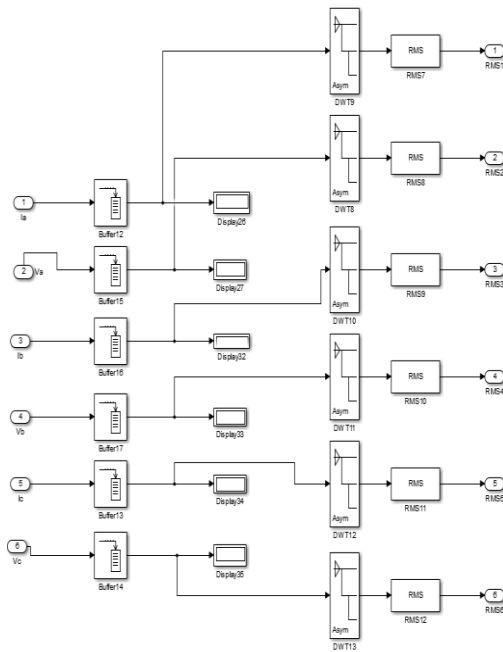


Figure 3.7: Signal transformation using DWT

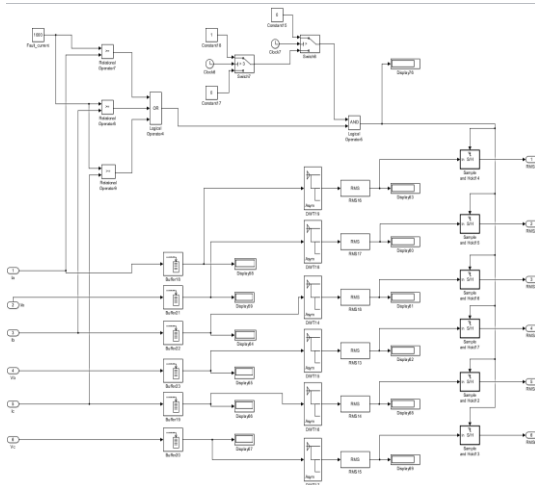


Figure 3.8: Fault feature extraction from the DWT

Artificial Neural Network Design

The artificial neural network used for the fault location in this study is based on a multilayer perceptron which consists of an input layer with neurons corresponding to the number of features of the fault signal and an output layer corresponding to the buses where faults can occur. The Pattern Recognition Neural Network App in Simulink is used for this purpose. To increase the accuracy of the fault location, the distribution network is divided into zones and sections with several neural networks being cascaded to locate the fault. The training data for the networks is a 6 x 154 matrix of numeric values consisting of the six fault features and 154 fault examples or scenarios. The examples comprise of the fault data obtained by simulating all the 11 fault types (a-b, b-c, a-c, a-g, b-g, c-g, a-b-g, b-c-g, a-c-g, a-b-c and a-b-c-g) on all the 14 lines. Equation 3.7 shows the number of examples.

$$\text{Number of examples} = 11 \times 14 = 154 \quad \dots 3.7$$

In the absence of more training data, these 154 rows of fault feature data are duplicated in order to obtain a much larger data set to obtain better training results. The total number of rows obtained after duplicating the data is 24,640. Appendix I and II present the original 154 rows of data and the corresponding target data.

First Level Artificial Neural Network Design

The first neural network at the top of the hierarchy is used to locate the Zone where the fault has occurred. There are two zones namely; Zone 1 and Zone 2. This neural network has six inputs which are the six features obtained from the outputs of the number of levels presented in equation 3.5. An input layer of 6 neurons, a hidden layer made up of 10 neurons and an output layer of 2 neurons are used in the design of the first neural network. The 2-neuron Output corresponds to the two zones of the network. Figures 3.9 and 3.10 show the neural network architecture. A 6 x 24,640 matrix of training data was used to train the ANN used to detect the zone where the fault occurred.

The target data for this ANN have the same number of rows as that of the training data but there are only two columns corresponding to the two Zones i.e. Zone 1 and Zone 2. A one (1) is placed in a row under a column corresponding to the zone where the fault occurred and a zero (0) elsewhere.

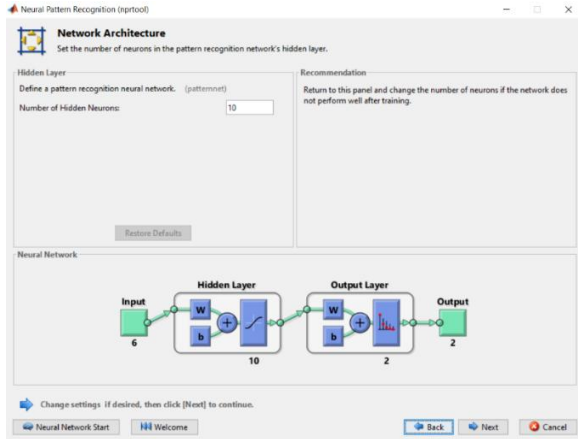


Figure 3.9: Zone Output Artificial Neural Network

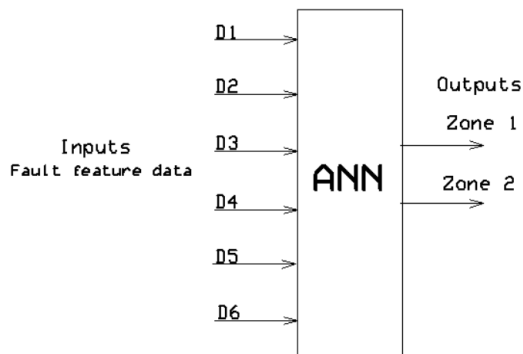


Figure 3.10: ANN for locating fault Zones

Second Level Artificial Neural Network Design

This set of neural networks in the hierarchy are two in number and their inputs are connected to the outputs of the first neural network as well as the original six fault data feature inputs. The original six (6) fault feature data and the zone fault indicator output from the first ANN thus make up a total of seven (7) inputs. The two Outputs of each of these two neural networks are the Sections 1 and 2 under each of the Zones. Figure 3.11 depicts this arrangement and Figures 3.12 and 3.13 shows the Simulink implementation.

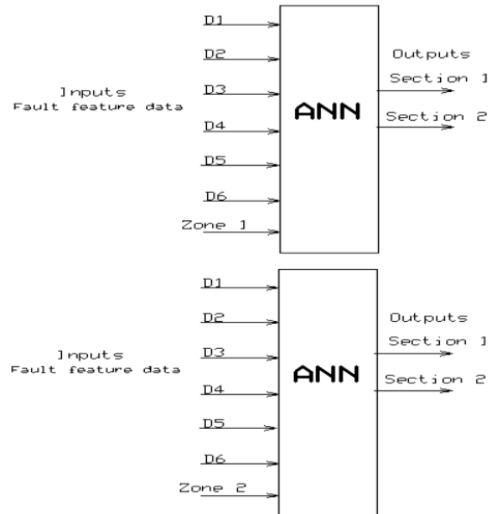


Figure 3.11: ANN for locating fault Sections

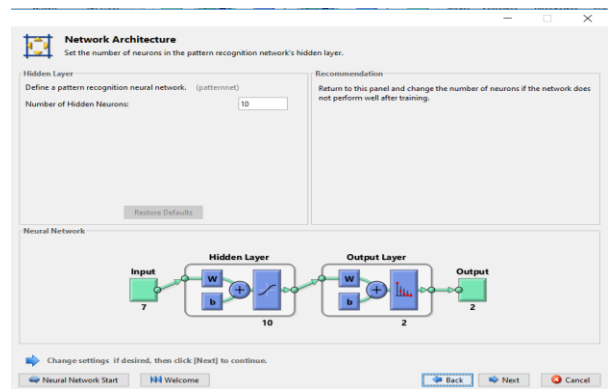


Figure 3.12: Simulink implementation for ANN for locating Zone 1 fault sections

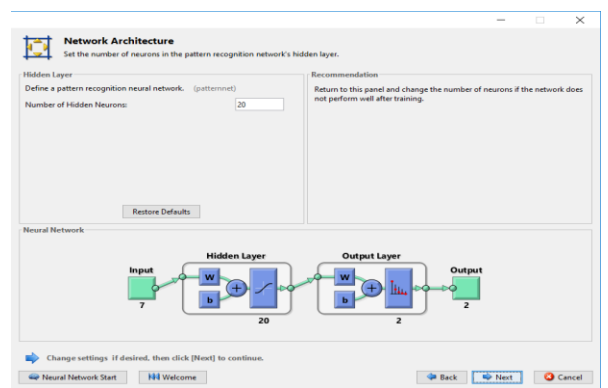


Figure 3.13: Simulink implementation for ANN for locating Zone 2 fault sections

The target data for this ANN have the same number of rows as that of the training data. There are two columns for each ANN corresponding to the two

Sections under each zone i.e. Section 1 and Section 2. A one (1) is placed in a row under a column corresponding to the section where the fault data corresponds to the faulty section and a zero (0) elsewhere.

Third Level Artificial Neural Network Design

For this set of neural networks in the hierarchy, there are four ANNs in number and their inputs are connected to the outputs of the first and second neural networks as well as the original six fault data feature inputs. The original six (6) fault feature data, the zone fault indicator output from the first ANN and the section fault indicator output from the second ANN thus make up a total of eight (8) inputs. The Outputs of each of these four neural networks are the lines under each of the Sections under the Zones. Figure 3.14 depicts this arrangement and Figures 3.15 to 3.18 show the Simulink implementation. Figure 3.19 shows the interconnection of all the neural networks put together to locate the faulty lines.

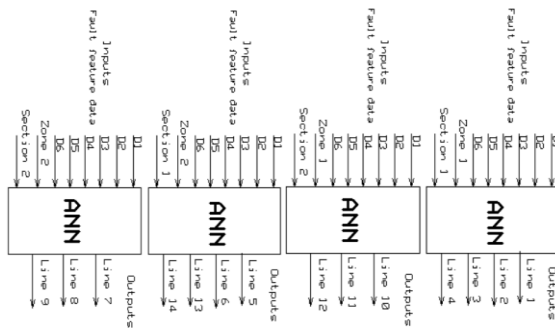


Figure 3.14: ANN for locating the faulty lines

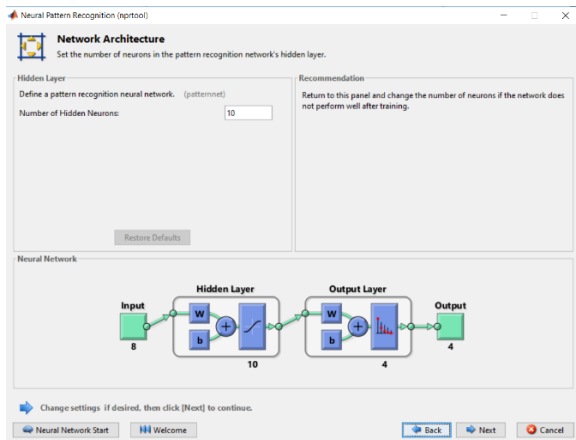


Figure 3.15: Simulink implementation of ANN for locating the faulty lines on Zone 1/Section 1

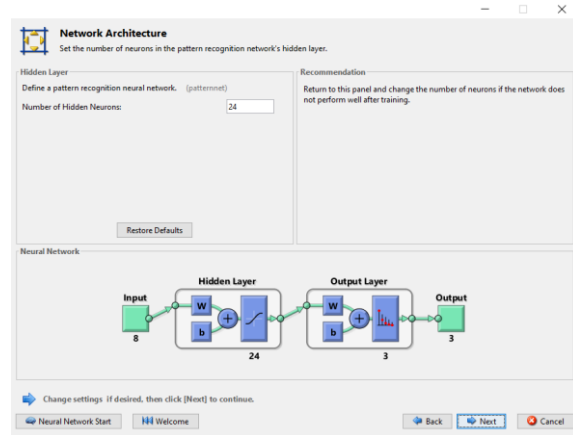


Figure 3.16: Simulink implementation of ANN for locating the faulty lines on Zone 1/Section 2

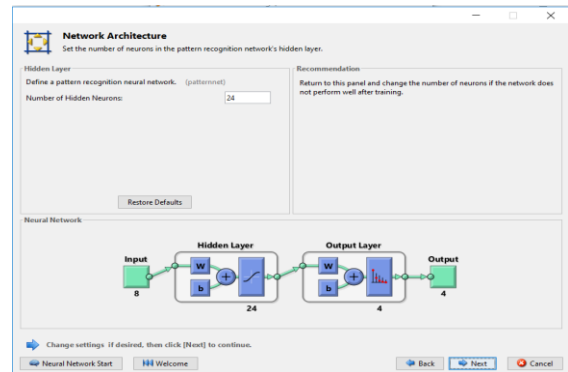


Figure 3.17: Simulink implementation of ANN for locating the faulty lines on Zone 2/Section 1

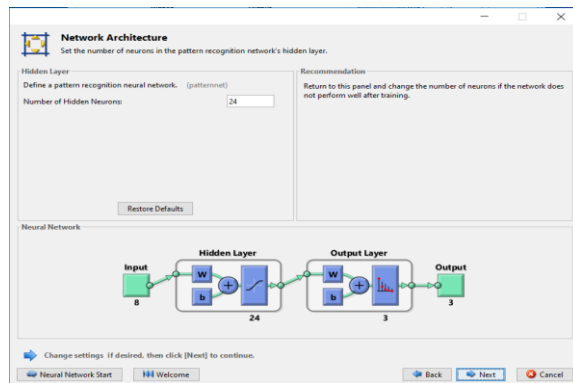


Figure 3.18: Simulink implementation of ANN for locating the faulty lines on Zone 2/Section 2

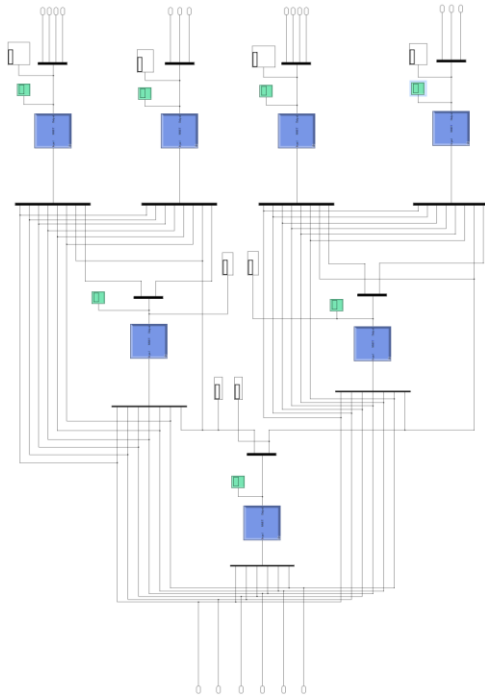


Figure 3.19: Integrated Artificial Neural Network Architecture implemented in Simulink

Fault Location Procedure

To locate a fault on the network, the fault must first be detected. The fault detection is carried out by the operation of the recloser upstream of the network which senses an abnormal current in the line and opens the line temporarily to clear the fault. The Sectionalizer logic monitors the current through it and waits for a response from the recloser. The Sectionalizer counts every reclose attempt and after one reclose attempt, the Sectionalizer isolates the faulty part of the network. A buffer implemented in Simulink is used to receive samples of the voltage and current waveforms of the signal. These samples are fed to the discrete wavelet transform (DWT) blocks which extracts the detail coefficients of the transformed signal. The root mean square (RMS) values of the coefficients corresponding to the fault signal are captured using the sample and hold blocks. Figure 3.8 depicts this arrangement. This sample period is from the inception of the fault up to the time the fault is isolated. The RMS values are the primary fault features that are fed to the artificial neural networks to locate the position of the fault on the network. Figure 3.20 and Figure 3.21 show the flow chart illustrating the fault detection and location algorithm respectively.

IV. DATA ANALYSIS AND FINDINGS

Recloser and Sectionalizer Testing Results

The figures presented in Figure 4.1 and Figure 4.2 are the transient waveforms of the currents and voltages caused by a fault. Figure shows the tripping of the feeder by the recloser three cycles after the fault has occurred and the isolation of the faulted portion of the network by the Sectionalizer once cycle after the first reclose attempt.

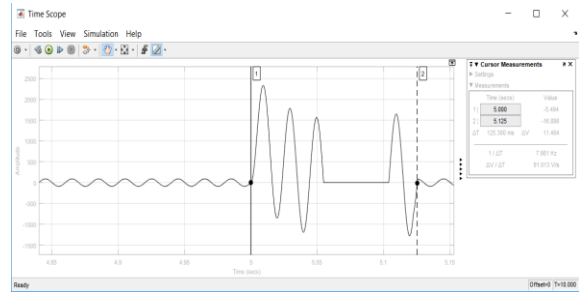


Figure 4.1: Transient current of network signal during faults

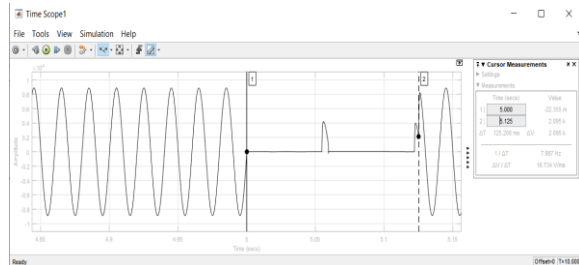


Figure 4.2: Transient voltage signal of network during fault

ANN Training Results

The Artificial Neural Networks (ANN) were trained using the “trainscg” function which is a network training function that updates weight and bias values according to the scaled conjugate gradient method. The following plots were obtained for each of the ANN trained and the codes used to generate them are presented in Appendix V to IX:

Network performance plot: A plot of Cross Entropy against Epochs that shows the training, validation and test progress. The Cross Entropy normally decreases as the number of iterations or epochs increase. The curve in this plot normally descends as the iterations increase and terminates where there is no further descent.

Neural network training state plot: This is a plot of the Gradient against Epochs as well as the Validation Fails against Epochs. The gradient decreases as the epochs increase and where the validation fails reach the maximum or where the training does not get better, the graph terminates.

Error histogram: This is a histogram of the Instances against Errors. It shows the errors that have occurred in the process and the frequency or the instances of the errors.

Confusion matrix: This is a matrix plot that shows the number of samples that were correctly classified as well as those that were incorrectly classified out of the total number of samples for the training, validation and testing phases. The boxes in red show the number of samples that were wrongly classified while those in the green boxes show the number of samples that were correctly classified.

Receiver operating characteristics plot (ROC): This is a plot of the True Positive Rate against the False Positive Rate. A line along the diagonal divides this graph into two; the left half and the right half. The more the ROC tends towards the upper left half of the plot, the more accurate the ANN is in classifying the data. This also shows the trade-off between correctly identifying positive cases and wrongly identifying negative cases.

A table summarizing the cross entropy (CE) and percentage errors for the training, validation and testing of the neural networks is also presented in tables 4.1, 4.2, 4.3, 4.4, 4.5, 4.6 and 4.7.

ANN Training Results for Locating Faults in Zones 1 and 2

The figures 4.3, 4.4, 4.5, 4.6 and 4.7 show the results from training the ANN that is used for locating the faults in Zone 1 and Zone 2.

Figure 4.3: Network performance plot for ANN locating faults in Zone 1 and Zone 2

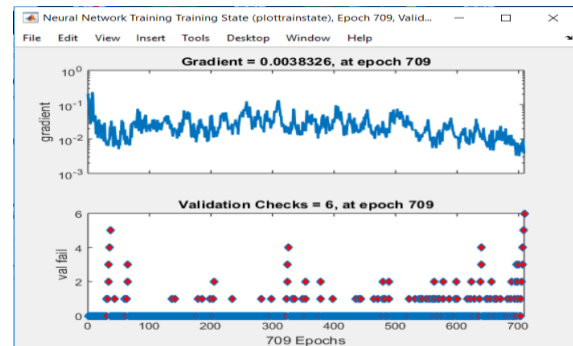


Figure 4.4: NN training state plot for ANN locating faults in Zone 1 and Zone 2

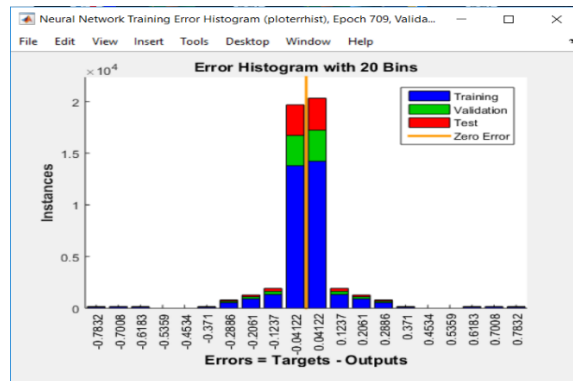
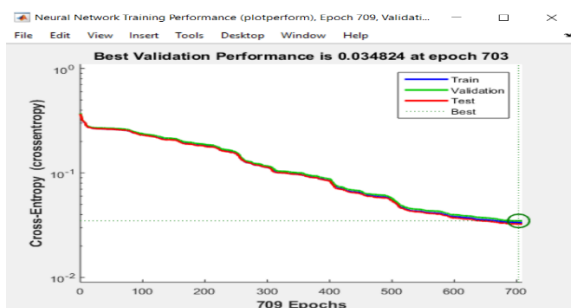


Figure 4.5: Error histogram for ANN for locating faults in Zone 1 and 2



Figure 4.6: Error Matrix for ANN locating faults in Zone 1 and 2



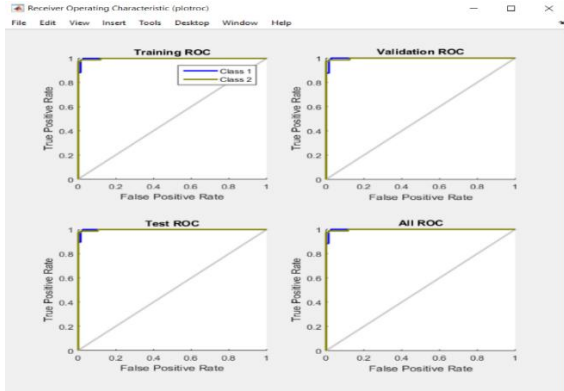


Figure 4.7: ROC for ANN Locating Faults in Zone 1 and 2

ANN Training Results for Locating Faults in Sections 1 and 2 of Zone 1

The figures 4.8, 4.9, 4.10, 4.11 and 4.12 show the results from training the ANN that is used for locating the faults on the lines of Section 1 and 2 of Zone 1.

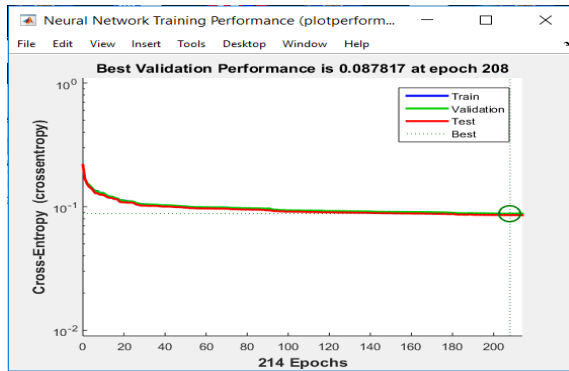


Figure 4.8: Network performance plot for ANN locating faults in Sections 1 and 2 of Zone 1

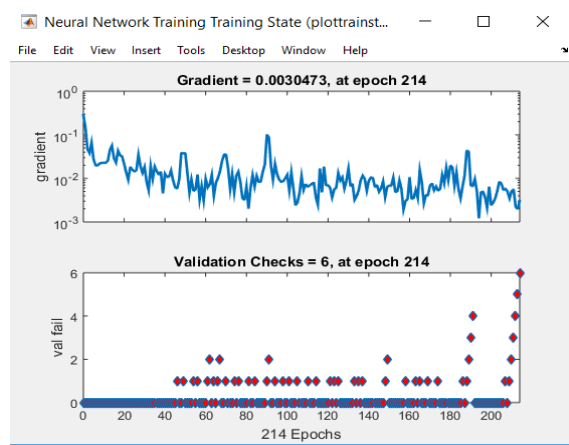


Figure 4.9: NN Training state for locating faults in Sections 1 and 2 of Zone 1

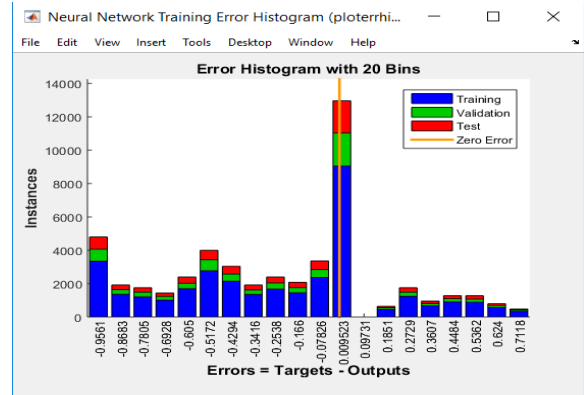


Figure 4.10: Error Histogram for ANN locating faults in Sections 1 and 2 of Zone 1



Figure 4.11: Confusion Matrix for ANN locating faults in Sections 1 and 2 of Zone 1

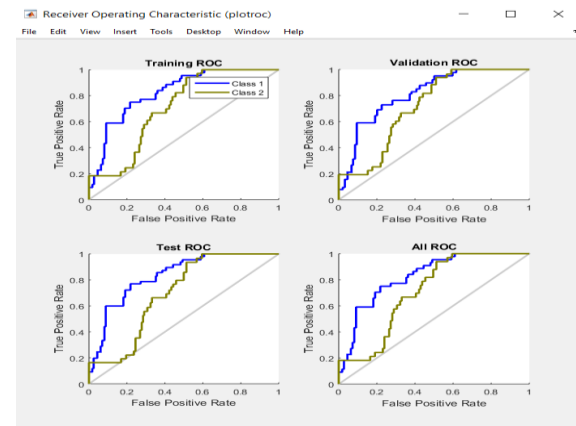


Figure 4.12: ROC for ANN locating faults in Sections 1 and 2 of Zone 1

ANN Training Results for Locating Faults in Sections 1 and 2 of Zone 2

The figures 4.13, 4.14, 4.15, 4.16 and 4.17 show the results from training the ANN that is used for locating the faults in Section 1 and Section 2 of Zone 2.

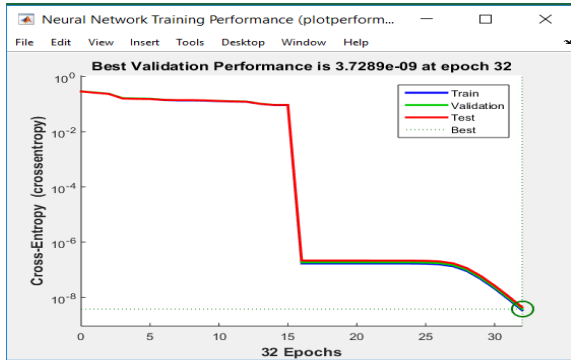


Figure 4.13: ANN Training Performance for locating faults in Sections 1 and 2 of Zone 2

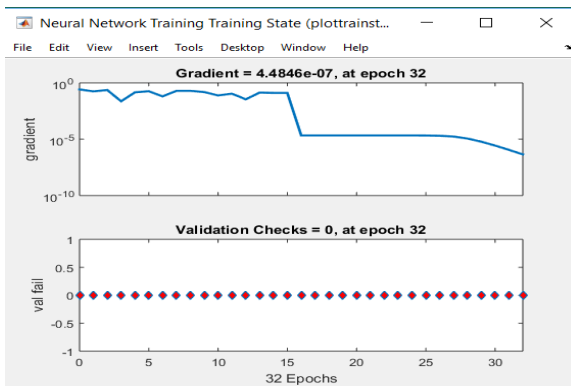


Figure 4.14: ANN Training State for locating faults in Sections 1 and 2 of Zone 2

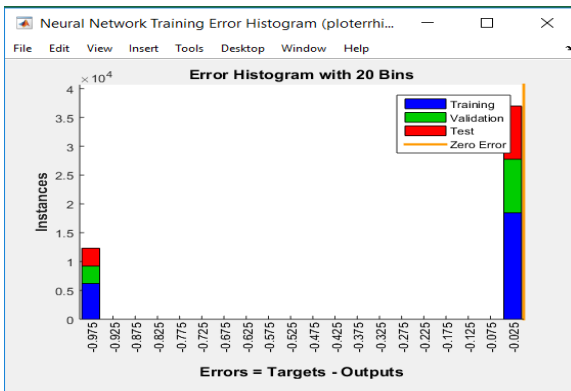


Figure 4.15: Error Histogram for ANN locating faults in Sections 1 and 2 of Zone 2

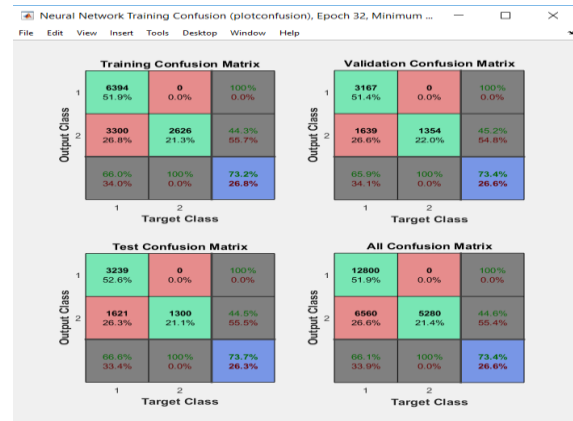


Figure 4.16: Confusion Matrix for ANN locating faults in Sections 1 and 2 of Zone 2

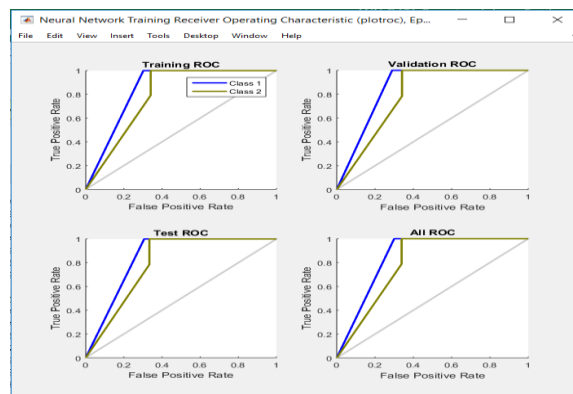


Figure 4.17: ROC for ANN locating faults in Sections 1 and 2 of Zone 2

ANN Training Results for Locating Faults on the Lines of Section 1 of Zone 1

The figures 4.18, 4.19, 4.20, 4.21 and 4.22 show the results from training the ANN that is used for locating the faults on the lines of Section 1 of Zone 1.

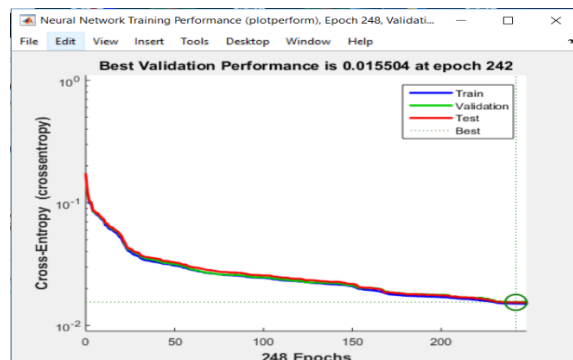


Figure 4.18: NN training performance for ANN locating faults on lines of section 1 of Zone 1

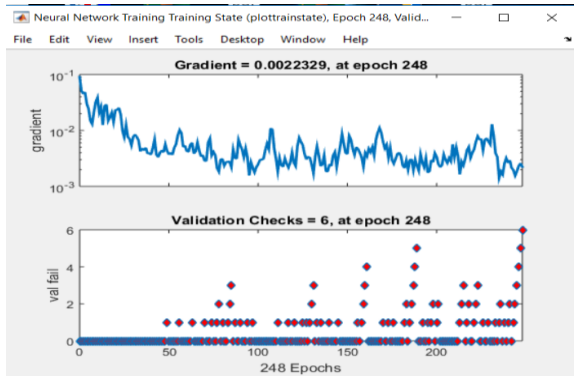


Figure 4.19: NN training state for ANN locating faults on lines of section 1 of Zone 1

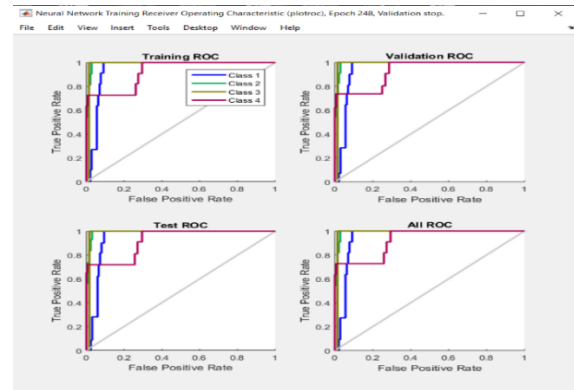


Figure 4.22: ROC for ANN locating faults on lines of section 1 of Zone 1

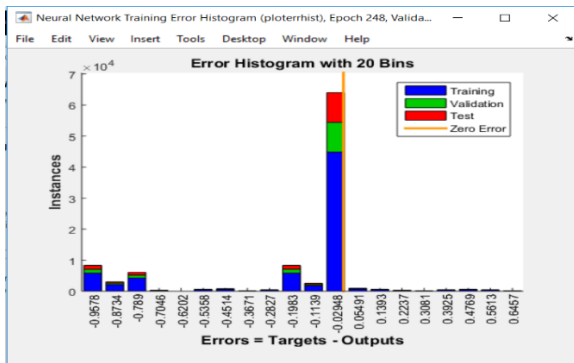


Figure 4.20: Histogram for ANN locating faults on lines of section 1 of Zone 1

ANN Training Results for Locating Faults on the lines of Section 2 of Zone 1

The figures 4.23, 4.24, 4.25, 4.26 and 4.27 show the results from training the ANN that is used for locating the faults on the lines of Section 2 of Zone 1.

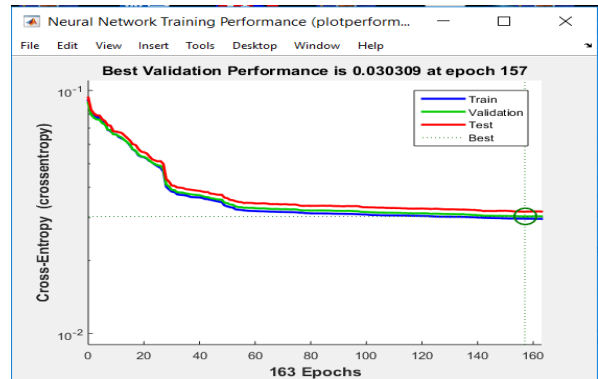


Figure 4.23: NN training performance for ANN locating faults on lines of section 2 of Zone 1



Figure 4.21: Confusion matrix for ANN locating faults on lines of section 1 of Zone 1

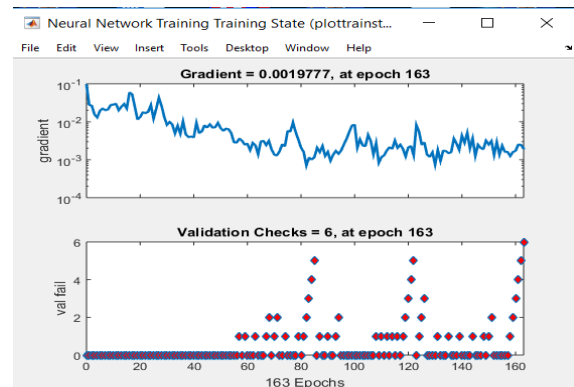


Figure 4.24: NN training state for ANN locating faults on lines of section 2 of Zone 1

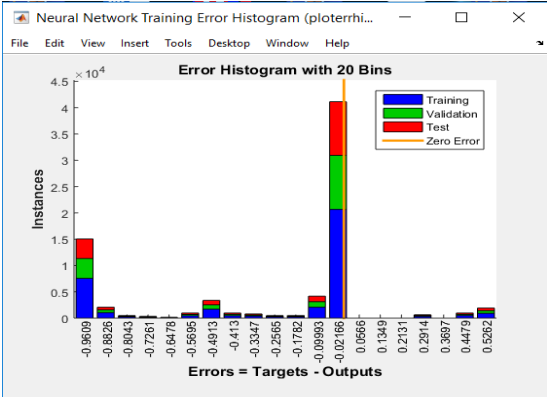


Figure 4.25: Error histogram for ANN locating faults on lines of section 2 of Zone 1

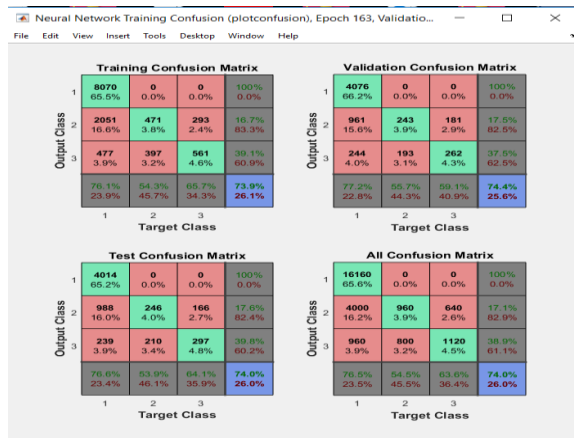


Figure 4.26: Confusion matrix for ANN locating faults on lines of section 2 of Zone 1

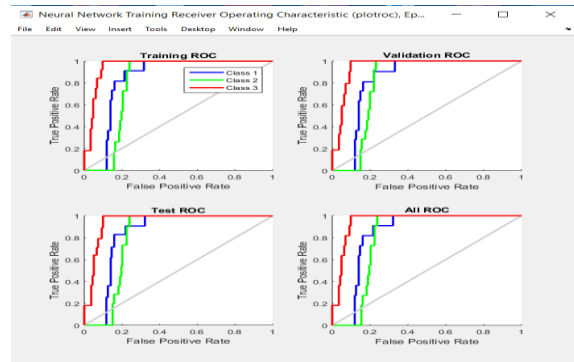


Figure 4.27: ROC for ANN locating faults on lines of section 2 of Zone 1

ANN Training Results for Locating Faults on the lines of Section 1 of Zone 2

The figures 4.28, 4.29, 4.30, 4.31 and 4.32 show the results from training the ANN that is used for locating the faults on the lines of Section 1 of Zone 2.

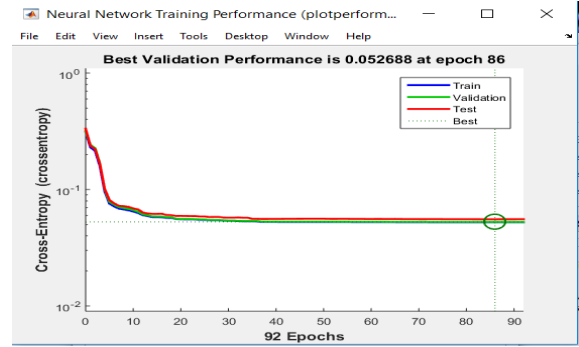


Figure 4.28: NN training performance for ANN locating faults on lines of section 1 of Zone 2

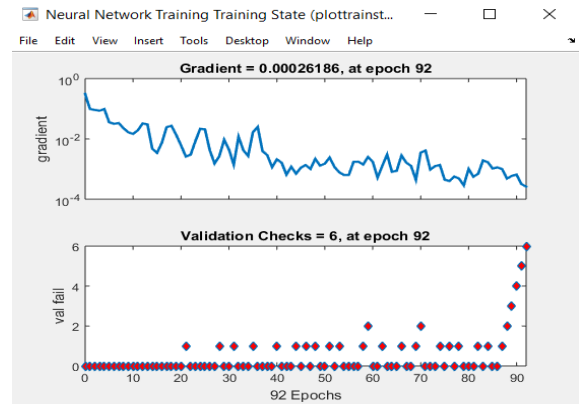


Figure 4.29: NN training state for ANN locating faults on lines of section 1 of Zone 2

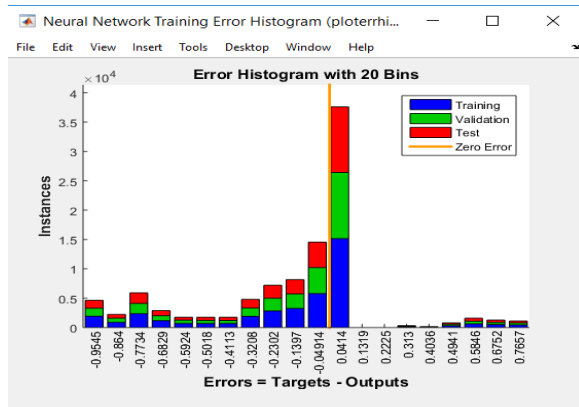


Figure 4.30: Error histogram for ANN locating faults on lines of section 1 of Zone 2



Figure 4.31: Confusion matrix for ANN locating faults on lines of section 1 of Zone 2

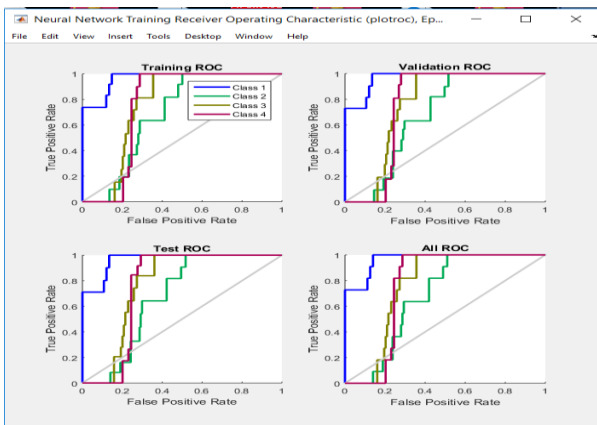


Figure 4.32: ROC for ANN locating faults on lines of section 1 of Zone 2

ANN Training Results for Locating Faults on the lines of Section 2 of Zone 2

The figures 4.33, 4.34, 4.35, 4.36 and 4.37 show the results from training the ANN that is used for locating the faults on the lines of Section 2 of Zone 2.

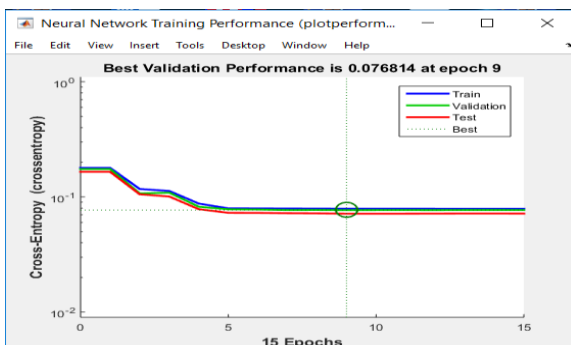


Figure 4.33: NN training performance for ANN locating faults on lines of section 2 of Zone 2

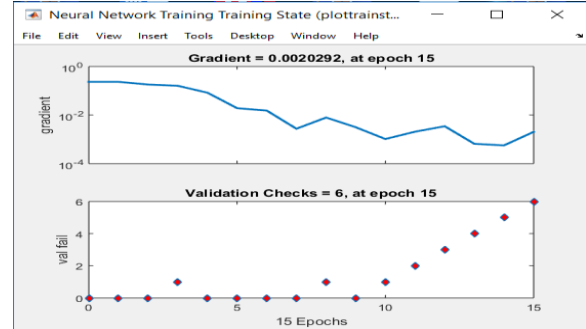


Figure 4.34: NN training state for ANN locating faults on lines of section 2 of Zone 2

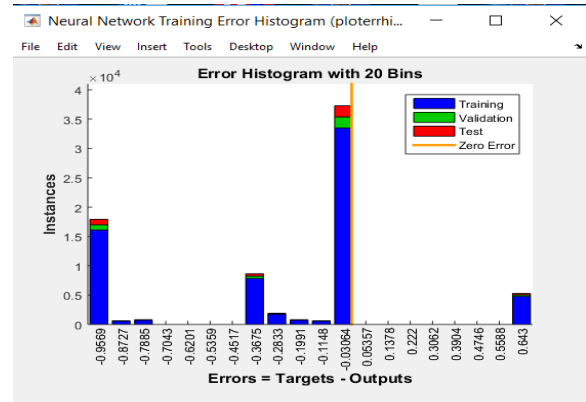


Figure 4.35: Error histogram for ANN locating faults on lines of section 2 of Zone 2

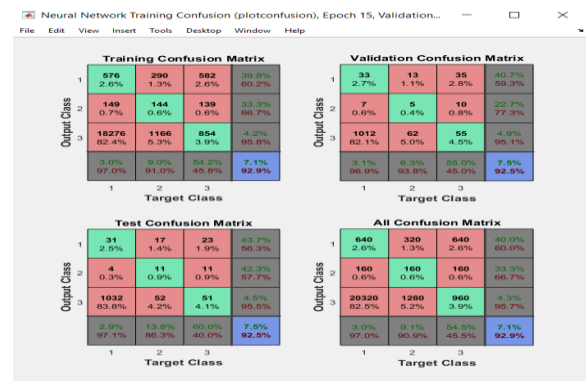


Figure 4.36: Confusion matrix for ANN locating faults on lines of section 2 of Zone 2

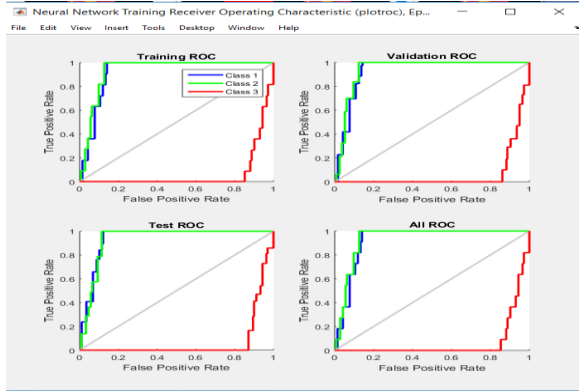


Figure 4.37: ROC for ANN locating faults on lines of section 2 of Zone 2

Summary of ANN Cross Entropy and Percent Error

The tables 4.1, 4.2, 4.3, 4.4, 4.5, 4.6 and 4.7 show the summary of the cross entropy and percent errors of all the artificial neural networks. The lower the cross-entropy error, the better the classification and a cross entropy error of zero means no error. The percent error indicates the fraction of samples which are misclassified. A value of zero (0) means no misclassifications while a value of 100 indicates maximum misclassifications.

Table 4.1: Summary of Cross Entropy and Percent Error for Zone 1 and 2 ANN

	Samples	%	Cross-Entropy Error (CE)	Percent Error (%E)
Training	17248	70	1.14385	1.97124
Validation	3696	15	3.19937	1.92099
Testing	3696	15	3.16956	1.86688

Table 4.2: Summary of Cross Entropy and Percent Error for Zone 1 ANN

	Sample s	%	Cross-Entropy Error (CE)	Percent Error (%E)
Training	17248	70	7.382531e-1	35.65630
Validatio n	3696	15	1.95092	34.87554
Testing	3696	15	1.93480	34.65909

Table 4.3: Summary of Cross Entropy and Percent Error for Zone 2 ANN

	Samples	%	Cross-Entropy Error (CE)	Percent Error (%E)
Training	12320	50	8.80625	25.11769
Validation	6160	25	13.21963	24.59415
Testing	6160	25	13.22172	25.17045

Table 4.4: Summary of Cross Entropy and Percent Error for Zone 1 Section 1 ANN

	Samples	%	Cross-Entropy Error (CE)	Percent Error (%E)
Training	17248	70	3.86760	39.01901
Validation	3696	15	10.96490	38.75811
Testing	3696	15	10.96562	38.89339

Table 4.5: Summary of Cross Entropy and Percent Error for Zone 1 Section 2 ANN

	Samples	%	Cross-Entropy Error (CE)	Percent Error (%E)
Training	12320	50	3.52081	44.91071
Validation	6160	25	5.31036	45.49512
Testing	6160	25	5.31789	45.20292

Table 4.6: Summary of Cross Entropy and Percent Error for Zone 2 Section 1 ANN

	Samples	%	Cross-Entropy Error (CE)	Percent Error (%E)
Training	9856	40	3.03916	45.71327
Validation	7392	30	3.56189	45.224561
Testing	7392	30	3.57743	45.33955

Table 4.7: Summary of Cross Entropy and Percent Error for Zone 2 Section 2 ANN

	Sample s	%	Cross- Entropy Error (CE)	Percent Error (%E)
Training	22176	90	3.39609e-1	53.67965
Validatio n	1232	5	2.53513	52.96266
Testing	1232	5	2.53495	52.23214

Fault Location Simulation Results

The table presented in table 4.8 shows the results obtained from simulating 20 faults randomly on the 15-bus distribution network. The fault location algorithm was able to locate the faulty line 60% of the time..

Table 4.8: Results obtained from randomly testing the fault location algorithm

Discussion of Results

The results presented in table 4.8 show a 60% accuracy level from a sample of 20 random trials carried out on different lines in the distribution network. This is a reflection of the level of accuracy obtained during the training, validation and testing of the artificial neural networks. The results obtained from the training, validation and testing of the neural networks gave different level of accuracies; some were more accurate than the others as shown in the results. The artificial neural network that performed the best during the training, validation and testing was the first level artificial neural network. This is the artificial neural network used to locate which of the two Zones has the faulty portion of the network. Figures 4.5, 4.6 and 4.7 show the very good results obtained from the training, validation and testing phases. This artificial neural network classifies the faulty Zone accurately with only 1% error.

From the random trials carried out, the lines connected to bus number 4 gave the highest number of errors as presented in table 4.8. The errors in locating the faulty lines in the network could be attributed to a number of

reasons. These could be as a result of noise in the data or the need to use a higher sampling frequency to increase the features of the data and thus the data size. A higher sampling frequency would increase the number of decompositions of the DWT and consequently the number of the detailed coefficients.

CONCLUSION

The reliability issues in power systems mainly come from faults on the distribution side of the grid. One way to improve reliability is by installing protection devices such as reclosers and Sectionalisers but permanent faults could still occur notwithstanding. When permanent faults occur, tracing the fault the traditional way can be burdensome, time consuming and prone to false reports. The traditional way of tracing the fault would typically involve the utility company receiving a call from a customer and dispatching a repair crew to locate the fault, clear the fault and restore power to the faulted part of the network. To further improve the reliability and save the cost and effort of dispatching a repair crew to locate the fault on the line, this project has presented a means of locating the fault using the recorded transient signal generated by the fault. This signal contains frequency components that are signature of the fault location and has been used to train artificial neural networks to identify the location on the line where the fault has occurred. Seven of these artificial neural networks have been cascaded in a hierarchical manner to improve the accuracy of locating the fault. The frequency components of the fault are extracted using the discrete wavelet transform which is a signal processing technique that is most suited to transient signals. The modelling and simulation of the fault location system is done in MATLAB/Simulink on a 15 bus IEEE distribution network with a grid supply and a distributed generator connected to the system. Twenty (20) random trials were conducted on different lines of the network and the fault location system was able to identify the faulty line 60% of the times.

REFERENCES

- [1] J. Euler-Chelpin, “Distribution Grid Fault Location: An Analysis of Methods for Fault

- Location in LV and MV Power Distribution Grids,” Uppsala University, Uppsala, 2018.
- [2] M. Safari, M. R. Haghifam and M. Zangiabadi, “A hybrid method for recloser and sectionalizer placement in distribution networks considering protection coordination, fault type and equipment malfunction,” *IET Generation, Transmission & Distribution*, vol. 15, p. 2176–2190, 2021.
- [3] B. Ghosh, C. A. K and B. A. R, “Reliability and efficiency enhancement of a radial distribution system through value-based auto-recloser placement and network remodelling,” *Protection and Control of Modern Power Systems*, vol. 8, no. 1, 2023.
- [4] Eaton, “Cooper Power Series,” July 2017. [Online]. Available: www.eaton.com/cooperpowerseries.. [Accessed 19 December 2023].
- [5] G&W Electric Company , “Diamondback® Switches Applied as Sectionalizers,” September 2019. [Online]. Available: <https://gwelec.com>. [Accessed 19 December 2023].
- [6] A. Jain, “Artificial Neural Network-Based Fault Distance Locator for Double-Circuit Transmission Lines,” *Advances in Artificial Intelligence*, 2013.
- [7] Z. Guo and F. Yan, “Fault Location for 10kV Distribution Line Based on traveling wave theory - DC Theory,” in *Power Engineering and Automation Conference (PEAM)*, Hebei province, 2011.
- [8] M. Saha, J. Izykowski and E. Rosolowski, *Fault Location on Power Networks*. Power Systems, Springer, 2010.
- [9] A. Yadav and A. S. Thoke, “Transmission line fault distance and direction estimation using artificial neural network,” *International Journal of Engineering, Science and Technology* , vol. 3, no. 8, pp. 110-121 , 2011.
- [10] T. Sangwan and N. Kumar, “A Comparative Study of Artificial Neural Networks for Fault Detection and Location in Mixed,” *EasyChair*, 2023.
- [11] A. A. Awalewa, P. O. Mbamaluikem and I. A. Samuel, “Artificial Neural Networks for Intelligent Fault Location on the 33-Kv Nigeria Transmission Line,” *International Journal of Engineering Trends and Technology* , vol. 54 , no. 3, pp. 147-155, 2017.
- [12] S. Jamali, A. Bahmanyar and S. Ranjbar, “Hybrid classifier for fault location in active distribution networks,” *Protection and Control of Modern Power Systems*, vol. 5, no. 17, 2020.
- [13] T. Bouthiba, “Artificial Neural Network-based Fault Location in EHV Transmission Lines,” *International Journal of Applied Mathematics and Computer Science*, vol. 14, no. 1, pp. 69-78, 2004.
- [14] A. Hadaeghi, M. M. Iliyaefar and A. A. Chirani, “Artificial Neural Network-based Fault Location in Terminal-hybrid High Voltage Direct Current Transmission Lines,” *International Journal of Engineering* , vol. 36, no. 02, pp. 215-225 , 2023.
- [15] M. H. Idris and M. R. Adzman, “Neural Network based Transmission Line Fault Classifier and Locator using Sequence Values,” *Journal of Physics: Conference Series*, 2022.
- [16] N. Ogar, S. Hussain and K. A. A. Gamage, “The use of artificial neural network for low latency of fault detection and localisation in transmission line,” *Heliyon* , 2023.
- [17] A. Yadav and S. Goad, “Fault Detection on Transmission Lines Using Artificial Neural Network,” *IJSART* , vol. 7, no. 9, pp. 335-339, 2021.
- [18] E. Bashier and M. Tayeb, “Faults Detection in Power Systems Using Artificial Neural Network,” *American Journal of Engineering Research* , vol. 02, no. 06, pp. 69-75 , 2013.
- [19] C. Zhou, S. Gui, Y. Liu, J. Ma and H. Wang, “Fault Location of Distribution Network Based on Back Propagation Neural Network Optimization Algorithm,” *Processes*, vol. 11, no. 1947, 2023.
- [20] S. S. Shingare, P. Khampariya and S. M. Bakre, “Efficient Fault Detection and Location in Extra High Voltage Networks: An Artificial Neural Network (ANN)-Based Approach,” *International Journal of Intelligent Systems and Applications in Engineering*, vol. 11, no. 3, p. 1051–1060 , 2023.

- [21] A. Mamo and A. Hizkiel, "Reliability assessment and enhancement of Dangila distribution system with distribution generation," *Cogent Engineering*, vol. 10, no. 1, 2023.
- [22] T. M. Aljohani and M. J. Beshir, "Distribution System Reliability Analysis for Smart Grid Applications," *Smart Grid and Renewable Energy*, vol. 8, pp. 240-251, 2017.
- [23] T. M. Aljohani and M. J. Beshir, "Matlab Code to Assess the Reliability of the Smart Power Distribution System Using Monte Carlo Simulation," *Journal of Power and Energy Engineering*, vol. 5, pp. 30-44, 2017.
- [24] MarkWide Research, "Recloser and Sectionalizer Market Analysis - Industry Size, Share, Research Report, Insights, Covid-19 Impact, Statistics, Trends, Growth and Forecast 2023 - 2030," MarkWide Research, Torrance, 2023.
- [25] N. D. Tleis, *Power Systems Modelling and Fault Analysis Theory and Practice*, Oxford : Elsevier, 2008.
- [26] J. Iżykowski, *Fault location on power transmission lines*, Wrocław : Oficyna Wydawnicza Politechniki Wrocławskiej, 2008.
- [27] J. Iżykowski, *Fault location on power transmission lines*, Wrocław: Oficyna Wydawnicza Politechniki Wrocławskiej, 2008.
- [28] M. Muniappan, "A comprehensive review of DC fault protection methods in HVDC transmission systems," *Protection and Control of Modern Power Systems*, vol. 6, no. 1, pp. 1-20, 2021.
- [29] U. Sahu, Y. Anamika and P. Mohammad, "A Protection method for multi-terminal HVDC system based on fuzzy approach," *MethodsX*, vol. 10, no. 102018, pp. 1-16, 2023.
- [30] A. Hadaeghi, I. M. M and A. A. Chirani, "Artificial Neural Network-based Fault Location in Terminal-hybrid High Voltage Direct Current Transmission Lines," *International Journal of Engineering*, vol. 36, no. 02, pp. 215-225, 2023.